Published October 26, 2009

Orientation of palmitoylated $Ca_V\beta2a$ relative to $Ca_V2.2$ is critical for slow pathway modulation of N-type Ca^{2+} current by tachykinin receptor activation

Tora Mitra-Ganguli,[1,2] Iuliia Vitko,[3] Edward Perez-Reyes,[3,4] and Ann R. Rittenhouse[1,2]

[1]Department of Physiology and [2]Program in Neuroscience, University of Massachusetts Medical School, Worcester, MA 01655
[3]Department of Pharmacology and [4]Neuroscience Graduate Program, University of Virginia, Charlottesville, VA 22908

The G_q-coupled tachykinin receptor (neurokinin-1 receptor [NK-1R]) modulates N-type Ca^{2+} channel ($Ca_V2.2$ or N channel) activity at two distinct sites by a pathway involving a lipid metabolite, most likely arachidonic acid (AA). In another study published in this issue (Heneghan et al. 2009. *J. Gen Physiol.* doi:10.1085/jgp.200910203), we found that the form of modulation observed depends on which $Ca_V\beta$ is coexpressed with $Ca_V2.2$. When palmitoylated $Ca_V\beta2a$ is coexpressed, activation of NK-1Rs by substance P (SP) enhances N current. In contrast, when $Ca_V\beta3$ is coexpressed, SP inhibits N current. However, exogenously applied palmitic acid minimizes this inhibition. These findings suggested that the palmitoyl groups of $Ca_V\beta2a$ may occupy an inhibitory site on $Ca_V2.2$ or prevent AA from interacting with that site, thereby minimizing inhibition. If so, changing the orientation of $Ca_V\beta2a$ relative to $Ca_V2.2$ may displace the palmitoyl groups and prevent them from antagonizing AA's actions, thereby allowing inhibition even in the presence of $Ca_V\beta2a$. In this study, we tested this hypothesis by deleting one (Bdel1) or two (Bdel2) amino acids proximal to the α interacting domain (AID) of $Ca_V2.2$'s I–II linker. $Ca_V\beta$s bind tightly to the AID, whereas the rigid region proximal to the AID is thought to couple $Ca_V\beta$'s movements to $Ca_V2.2$ gating. Although Bdel1/β2a currents exhibited more variable enhancement by SP, Bdel2/β2a current enhancement was lost at all voltages. Instead, inhibition was observed that matched the profile of N-current inhibition from $Ca_V2.2$ coexpressed with $Ca_V\beta3$. Moreover, adding back exogenous palmitic acid minimized inhibition of Bdel2/β2a currents, suggesting that when palmitoylated $Ca_V\beta2a$ is sufficiently displaced, endogenously released AA can bind to the inhibitory site. These findings support our previous hypothesis that $Ca_V\beta2a$'s palmitoyl groups directly interact with an inhibitory site on $Ca_V2.2$ to block N-current inhibition by SP.

INTRODUCTION

Exogenously applied arachidonic acid (AA) or stimulation of certain G_q-coupled receptors (G_qPCRs) enhances as well as inhibits N current (Barrett et al., 2001; Liu et al., 2001; Liu and Rittenhouse, 2003a; and see Heneghan et al. in this issue). In Heneghan et al. (2009), we found that the form of modulation observed depends on which accessory $Ca_V\beta$ subunit is coexpressed with $Ca_V2.2$. When $Ca_V\beta1b$, $Ca_V\beta3$, or $Ca_V\beta4$ is present, AA (or receptor agonist) rapidly enhances N current; however, enhancement quickly progresses to robust inhibition. In contrast, currents from $Ca_V\beta2a$-containing channels exhibit sustained enhancement. Of the known $Ca_V\beta$ subunits, only $Ca_V\beta2a$ is palmitoylated on its two N-terminal cysteine residues (Chien et al., 1996; Takahashi et al., 2003). We hypothesized that persistent enhancement may result from the palmitoyl groups of $Ca_V\beta2a$ assuming a position within the membrane that prevents AA from interacting with the N channel's inhibitory sites. In support of this possibility, we found that AA no longer enhanced but instead inhibited N current from channels containing a depalmitoylated $Ca_V\beta2a$ ($Ca_V\beta2a$(C3,4S); Chien et al., 1996). Additionally, when $Ca_V\beta2a$'s N terminus was substituted into $Ca_V\beta1b$ to form the chimera $Ca_V\beta2a$/β1b (Chien et al., 1998), N current was no longer inhibited, but instead enhancement was observed, which is consistent with the palmitoyl groups preventing inhibition. Lastly, exogenously applied palmitic acid successfully minimized the inhibition normally observed with $Ca_V\beta3$. Collectively, these findings suggest that the palmitoyl groups are sufficient for preventing N-current inhibition by the slow pathway. This signal transduction cascade is initiated by G_qPCRs that use PIP_2 breakdown (Wu et al., 2002; Gamper et al., 2004), resulting in release of a free fatty acid, most likely AA

Correspondence to Ann R. Rittenhouse: Ann.Rittenhouse@umassmed.edu

T. Mitra-Ganguli's present address is McGovern Institute for Brain Research, Massachusetts Institute of Technology, Cambridge, MA 02139.

Abbreviations used in this paper: AA, arachidonic acid; AID, α interacting domain; BiFC, bimolecular fluorescence complementation; CFP, cyan fluorescent protein; HEK, human embryonic kidney; M_1R, M_1 receptor; NK-1R, neurokinin-1 receptor; SP, substance P; TTP, time to peak; wt, wild type.

© 2009 Mitra-Ganguli et al. This article is distributed under the terms of an Attribution–Noncommercial–Share Alike–No Mirror Sites license for the first six months after the publication date (see http://www.jgp.org/misc/terms.shtml). After six months it is available under a Creative Commons License (Attribution–Noncommercial–Share Alike 3.0 Unported license, as described at http://creativecommons.org/licenses/by-nc-sa/3.0/).

The Rockefeller University Press $30.00
J. Gen. Physiol. Vol. 134 No. 5 385–396
www.jgp.org/cgi/doi/10.1085/jgp.200910204

Supplemental Material can be found at:
http://jgp.rupress.org/content/suppl/2009/10/26/jgp.200910204.DC1.html

The Journal of General Physiology

Downloaded from jgp.rupress.org on May 20, 2011

Published October 26, 2009

(Liu and Rittenhouse, 2003a; Liu et al., 2006; Heneghan et al., 2009).

From these findings, we proposed the following model to explain loss of inhibition in the presence of $Ca_V\beta2a$: AA is released after G_qPCR stimulation of phospholipid breakdown (Fig. 1 A). Once released, AA normally binds to an inhibitory site on the channel. However, when $Ca_V\beta2a$ is present, its palmitoyl groups occupy the inhibitory site blocking AA's interaction with $Ca_V2.2$ (Fig. 1 B). For the palmitoyl groups of $Ca_V\beta2a$ to interact with a specific site on $Ca_V2.2$, we predicted that $Ca_V\beta2a$ must reside in a specific orientation so that the palmitoyl groups situate close to or overlapping with the channel's inhibitory site. To determine whether such an interaction might occur, in this study we tested whether changing $Ca_V\beta2a$'s orientation relative to $Ca_V2.2$ rescues inhibition.

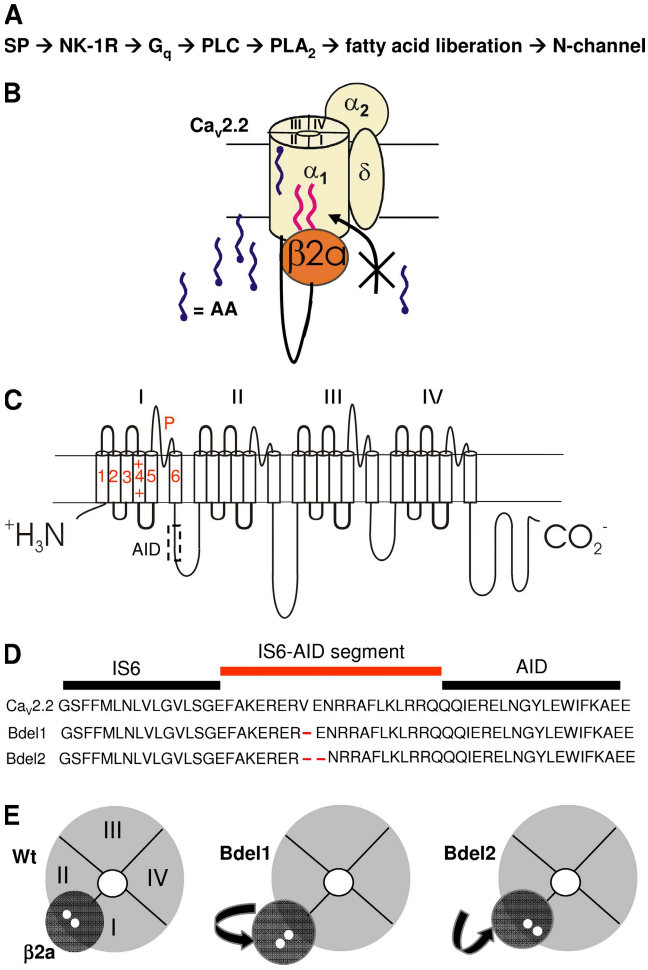


Figure 1. $Ca_V2.2$ model system to be tested by NK-1R activation. (A) Flow chart representing the signaling cascade used by SP to modulate N current. (B) Schematic of model to be tested: N channels consist of the pore-forming $Ca_V2.2$, which is made up of four homologous domains (I–IV) also referred to as pseudosubunits, $\alpha_2\delta$-1, and a $Ca_V\beta$. Palmitoylated $Ca_V\beta2a$ blocks endogenously liberated free AA from binding to $Ca_V2.2$'s inhibitory sites after exposure of cells to SP. AA's enhancement site remains available and is shown here in the outer regions of $Ca_V2.2$, although the actual location of this site remains uncharacterized. (C) Topological organization of $Ca_V2.2$ showing the six transmembrane segments and pore loop (P) of each pseudosubunit. An intracellular linker tethers each pseudosubunit to the subsequent one. $Ca_V\beta$ binds the AID region on the I–II linker at a site (delineated by the dotted box) that overlaps with a binding site for Gβγ. (D) The amino acid deletions in the region proximal to the AID result in Bdel1 and Bdel2 mutant channels. (E) Cross-sectional views from the inner pore region of wt $Ca_V2.2$ and the two mutant channels. Sequential amino acid deletions in the IS6-AID segment of Bdel1 and Bdel2 are predicted to reorient $Ca_V\beta2a$ such that the two palmitoyl groups (small white circles) are displaced from their wt positions.

All $Ca_V\beta$s bind with high affinity to the cytoplasmic linker between domains I and II (Fig. 1 C) at the α interacting domain (AID; Pragnell et al., 1994; Chen et al., 2004; Opatowsky et al., 2004; Van Petegem et al., 2004). The region proximal to the AID appears to couple $Ca_V\beta$'s movements to tune the gating properties of the channel, possibly by modulating the movements of IS6 (Vitko et al., 2008; Zhang et al., 2008). This IS6-AID segment appears to form, in part, a rigid helical structure that regulates the orientation of $Ca_V\beta2a$ and consequently its secondary interactions with $Ca_V2.2$. Deleting one (Bdel1) or two (Bdel2) amino acids in the IS6-AID segment (Fig. 1 D) changes the orientation of $Ca_V\beta2a$ to $Ca_V2.2$ (Fig. 1 E) with each shift in the helix (Vitko et al., 2008). Therefore, we tested Bdel1 and Bdel2 mutants coexpressed with $Ca_V\beta2a$ for sensitivity to substance P (SP). Bdel1 exhibited minimal current enhancement, whereas Bdel2 rescued current inhibition by the slow pathway. In turn, exogenous palmitic acid reduced this inhibition. These findings are consistent with a model in which the orientation of a palmitoylated cytoplasmic protein, $Ca_V\beta2a$, alters the regulation of the transmembrane protein, $Ca_V2.2$. This model raises the possibility that other cytosolic proteins may use their palmitoyl groups to interact with transmembrane segments of associated proteins to modify their behavior.

MATERIALS AND METHODS

Site-directed mutagenesis

The cDNA encoding the rat brain $Ca_V2.2$ (GenBank/EMBL/DDBJ accession no. AF055477) was subcloned into the plasmid vector pcDNA6 (Lin et al., 1997) and was provided by D. Lipscombe (Brown University, Providence, RI). To make the mutant Bdel1 and Bdel2 cDNAs, a 1.5-kb fragment was subcloned into pCR2.1-TOPO (Invitrogen) and mutated using the QuikChange protocol and Pfu Ultra DNA polymerase (Agilent Technologies). Oligonucleotide primers, which were obtained from Invitrogen, were used without purification. All restriction enzymes were purchased from New England Biolabs, Inc. The full-length cDNA was reassembled in the original plasmid vector that was cut with AscI and BsiWI by ligating the following fragments: AscI(32)–BlpI(355), BlpI–SacI(1407), and SacI–BsiWI(2991). The Bdel1 and Bdel2 amino acid deletions were contained in the BlpI–SacI fragment. The sequence of this fragment was verified for each mutant by automated sequencing at the University of Virginia Biomolecular Research Facility.

Downloaded from jgp.rupress.org on May 20, 2011

Published October 26, 2009

Transfection

Human embryonic kidney (HEK) cells with a stably transfected M_1 receptor (M_1R; HEK-M1) were grown at 37°C with 5% CO_2 in Dulbecco's modified Eagle's medium/F12 supplemented with 10% FBS, 1% G418, 0.1% gentamicin, and 1% HT supplement (Invitrogen). For transfection, cells were plated in 12-well plates at 50–80% confluency. Cells were transiently transfected using Lipofectamine PLUS reagent (Invitrogen) as per the manufacturer's instructions. The transfection mixture consisted of plasmids encoding wild-type (wt) or mutant $Ca_v2.2$ e[a10, Δ18a, Δ24a, 31a, 37b, 46] (GenBank accession no. AF055477; Fig. 1, C and D; Vitko et al., 2008), $\alpha_2\delta$-1 (GenBank accession no. AF286488), and either $Ca_V\beta$2a (GenBank accession no. M80545) or $Ca_V\beta$3 (GenBank accession no. M88751) at a 1:1:1 molar ratio. 28 ng/well of plasmid encoding neurokinin-1 receptor (NK-1R; GenBank accession no. AY462098; UMR cDNA Resource Center, University of Missouri, Rolla, MO) and enhanced green fluorescent protein cDNA (used at <10% of total cDNA) were also included in the transfection medium. Cells were plated on poly-L-lysine–coated coverslips 24–72 h after transfection. However, currents elicited from Bdel1 and Bdel2 mutants were not detectable. To boost mutant channel expression by increasing transcription, 80 ng of plasmid containing the SV40 T antigen was included during transfection. Currents were recorded between 24 and 76 h after transfection.

Electrophysiology

Whole-cell Ba^{2+} currents were recorded at room temperature (20–24°C) using a patch-clamp amplifier (model 3900a; Dagan Instruments Inc.). Currents were filtered at 1–5 kHz using the amplifier's four-pole low-pass Bessel filter and digitized at 20 kHz with a micro1401 interface (Cambridge Electronic Design [CED]). Data were acquired and analyzed using either IPLab 4.0 (Scanalytics) as described previously (Vitko et al., 2007) or Signal 2.16 (CED) and stored on a personal computer. Before analysis, capacitive and leak currents were subtracted using a scaled-up hyperpolarizing test pulse to −100 mV. For all recordings, cells were held at −90 mV and given either a 24- or 100-ms depolarization to the test pulse indicated. Unless mentioned, the protocol was repeated every 4 s. For prepulse experiments, a 24-ms depolarization (P1) was followed 250 ms later by a step depolarization to 120 mV for 25 ms, then followed 30 ms later by another 24-ms depolarization (P2) and repeated every 10 s (Fig. 2 C). Electrodes were pulled from borosilicate glass capillary tubes. Each electrode was fire polished to ∼1 µm to yield pipettes with resistances of 2–3 MΩ. The external solution contained 125 mM NMG-aspartate, 10 mM HEPES, and 5 or 20 mM barium (Ba^{2+}) acetate; pH was adjusted to 7.5 with CsOH. When the Ba^{2+} concentration was lowered from 20 to 5 mM (for recording wt $Ca_v2.2$ currents), 135 mM NMG-aspartate was substituted for Ba^{2+}. The internal solution of the pipette consisted of 135 mM Cs-aspartate, 10 mM HEPES, 0.1 mM 1,2-bis(*O*-aminophenoxy) ethane-*N*,*N*,*N*′,*N*′-tetraacetic acid (BAPTA), 5 mM $MgCl_2$, 4 mM ATP, and 0.4 mM GTP; the pH was adjusted to 7.5 with CsOH. When 20 mM BAPTA was included in the pipette solution, the Cs-aspartate concentration was lowered accordingly in the internal solution.

Bimolecular fluorescence complementation (BiFC)

BiFC imaging was performed as previously described (Vitko et al., 2008). In brief, a small C-terminal (amino acids 159–238) sequence of cyan fluorescent protein (CFP) was fused to the C terminus of full-length $Ca_V\beta$2a (Fig. S1 A). The big N-terminal fragment of CFP (amino acids 1–158) was fused to the N terminus of $Ca_V2.2$, Bdel1, or Bdel2. Plasmids encoding 250 ng $Ca_V2.2$, Bdel1, or Bdel2, 1 µg $\alpha_2\delta$-1, and 1 µg of full-length β2a were transiently transfected into HEK-293 cells. After 18 h, the cells were plated onto poly-L-lysine–treated glass-bottom dishes (Fluorodish; World Precision Instruments). BiFC was visualized by cyan fluorescence signals that were collected with IPLab software and a Sensicam QE (Cooke) mounted on a microscope (100× objective and 2 × 2 binning; IX61; Olympus) equipped with a confocal spinning disk unit (Olympus). Digital images were background subtracted using a region devoid of cells.

Pharmacology

SP was prepared as a 0.5-mM stock solution in 0.05 M acetic acid and stored at −20°C. To make a working concentration of 5 nM, the stock was serially diluted with bath solution daily. Palmitic acid was dissolved in 100% ethanol to make a stock solution. Working solutions were made by diluting the stock 1:1,000 with bath solution. BSA (fraction V, heat shock, fatty acid ultra free; Roche) was dissolved in the bath solution and diluted further to make a final concentration of 1 mg/ml. All chemicals were obtained from Sigma-Aldrich except where noted. Drugs were applied with a gravity-driven perfusion system, and complete bath exchange was achieved within 10–14 s.

Data analysis

After the onset of the test pulse, maximal inward current of whole-cell traces was measured using a trough-seeking function. Percent change in current amplitude was measured as $[(I - I')/I] \times 100$, where I is the mean amplitude of peak current measured from five current traces before drug application and I' is the mean current amplitude measured from five current traces at least 2 min after application of SP, unless otherwise noted.

Statistical analysis

Summary data are presented as mean ± SEM. Mean current amplitude before and after application of SP was compared using a two-tailed paired *t* test. Two means were compared using a two-way Student's *t* test. Statistical significance was set at $P < 0.05$. Data were analyzed using Excel (Microsoft) and Origin (OriginLab).

Online supplemental material

Fig. S1 shows BiFC images of $Ca_V2.2$, Bdel1, and Bdel2 colocalizing with $Ca_V\beta$2a to the plasma membrane. Online supplemental material is available at http://www.jgp.org/cgi/content/full/jgp.200910204/DC1.

RESULTS

SP enhances wt $Ca_v2.2$ current via a BAPTA-sensitive, voltage-independent pathway

We characterized several biophysical properties of N-current enhancement by SP. In HEK-M1 cells transfected with $Ca_V2.2$, $Ca_V\beta$2a, $\alpha_2\delta$-1, and the NK-1R, we first tested whether as with inhibition, the enhancement of N current occurs via a BAPTA-sensitive pathway. In cells dialyzed with a low (0.1 mM) BAPTA concentration, application of 5 nM SP enhanced N current 62 ± 18% (Fig. 2, A [left] and B). In contrast, when cells were dialyzed with a high (20 mM) BAPTA concentration for at least 2 min to chelate intracellular Ca^{2+}, SP no longer elicited current modulation (Fig. 2, A [right] and B). Thus, enhancement involves a BAPTA-sensitive pathway similar to that shown earlier for M_1R-mediated N-current inhibition (Beech et al., 1991; Bernheim et al., 1991; Mathie et al., 1992; Liu et al., 2001; Liu and Rittenhouse, 2003a).

Downloaded from jgp.rupress.org on May 20, 2011

Published October 26, 2009

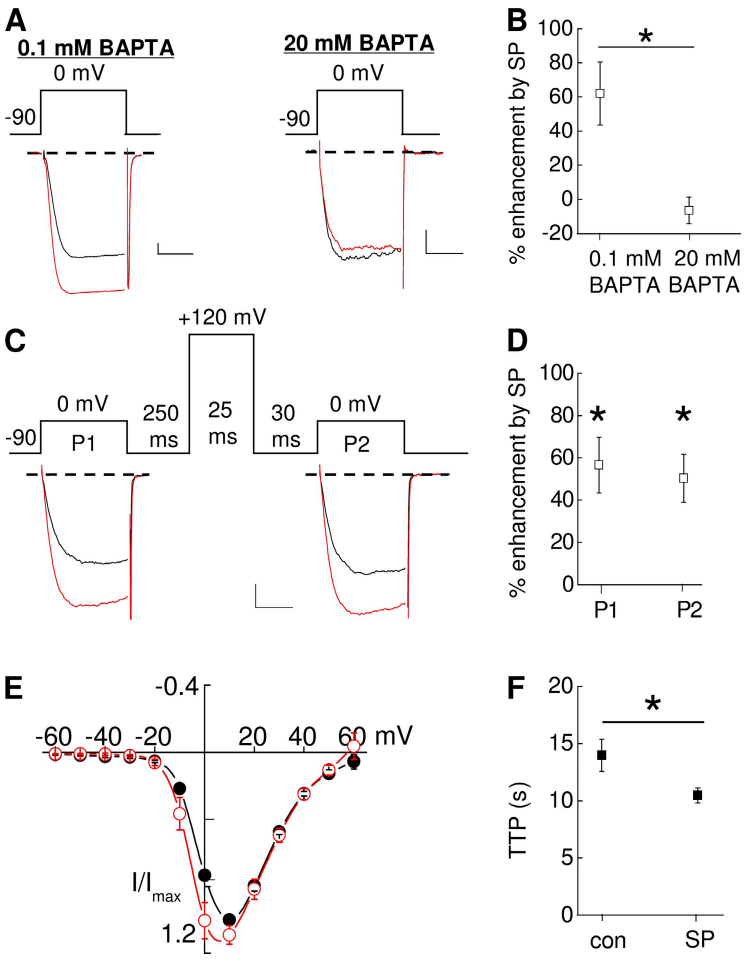


Figure 2. NK-1R activation enhances $Ca_V2.2/Ca_V\beta2a$ currents. HEK-M1 cells were transiently transfected with $Ca_V2.2$, $\alpha_2\delta$-1, β2a, and NK-1R. (A) Individual traces taken before and 2 min after application of 5 nM SP. (left) 0.1 mM BAPTA was present in the internal solution. (right) 20 mM BAPTA in the internal solution. (B) Comparison of the mean percent enhancement for cells dialyzed with 0.1 or 20 mM BAPTA (n = 4–9); *, $P < 0.05$ compared with inhibition in the presence of 0.1 mM BAPTA. (C) Individual traces taken before and 2 min after application of SP. P1 and P2 represent current measured before and after a prepulse, respectively. (D) Summary of the percent enhancement by SP at 0 mV before and after a prepulse (n = 9); *, $P < 0.05$ compared with P1 and P2 control currents before SP application. (E) Averaged current–voltage relationships measured before (closed circles) and after (open circles) application of SP. (F) Summary of TTP before and after application of SP (n = 6); *, $P < 0.05$ compared with control. Error bars represent SEM. Bars, 10 ms and 200 pA.

Second, we tested whether enhancement, as with inhibition, is insensitive to prepulse facilitation of current. Similar to our previous studies using exogenously applied AA (Barrett et al., 2001; Liu et al., 2001), M_1R agonist (Liu and Rittenhouse, 2003a), or SP activation of NK-1Rs (Heneghan et al., 2009), current enhancement occurred between −10 and 0 mV (Fig. 2, C–E). Current–voltage (I-V) plots revealed that maximal enhancement occurred 10 mV negative to the voltage that elicited peak inward current—in this case at 0 mV (Fig. 2 E). Thus, we measured N current over time by stepping to a test potential 10 mV to the left of where maximal inward current occurs. Using this protocol, a slight relief from tonic inhibition was observed under control conditions; however, after SP application, both P1 and P2 currents exhibited similar significant ($P < 0.05$) enhancement (62 ± 18% and 50 ± 11%, respectively) compared with control currents (Fig. 2, C and D).

AA-induced enhancement of N current coincides with an increased rate of activation in SCG neurons (Barrett et al., 2001). Therefore, in a third study, we examined whether enhancement by SP involves an increase in activation kinetics, detected as a change in time to peak (TTP) inward current. We measured the TTP of N current before and after application of SP. As shown in Fig. 2 F, SP significantly decreased TTP ($P < 0.05$; n = 6) when $Ca_V\beta2a$ was coexpressed with $Ca_V2.2$ similar to native N current (Barrett et al., 2001). Collectively, these tests indicate that in addition to recapitulating the properties of native N-current enhancement, recombinant N-current enhancement exhibits similar properties to N-current inhibition by SP: sensitivity to the internal BAPTA concentration but unaltered by prepulses.

Modulation of Bdel1 current by SP is disrupted

We next examined whether mutant $Ca_V2.2$ channels coexpressed with $Ca_V\beta2a$ exhibit similar modulation by SP. Bdel1 has a single amino acid deletion in the IS6-AID segment (Vitko et al., 2008) that reorients $Ca_V\beta2a$'s position relative to Bdel1 (Fig. 1, D and E). We hypothesized that this deletion may sufficiently move $Ca_V\beta2a$ such that the palmitoyl groups no longer occupy the putative inhibitory site so that SP will now inhibit rather than enhance current. Although SP enhanced Bdel1 currents in seven of seven cells (Fig. 3 A), enhancement varied from as little as 12% to as high as 135% and thus was not significant (Fig. 3, B and C). To rule out the possibility that inhibition was disrupted as a result of a change in the inhibitory site, we tested Bdel1 coexpressed with $Ca_V\beta3$ for modulation by SP.

Downloaded from jgp.rupress.org on May 20, 2011

Published October 26, 2009

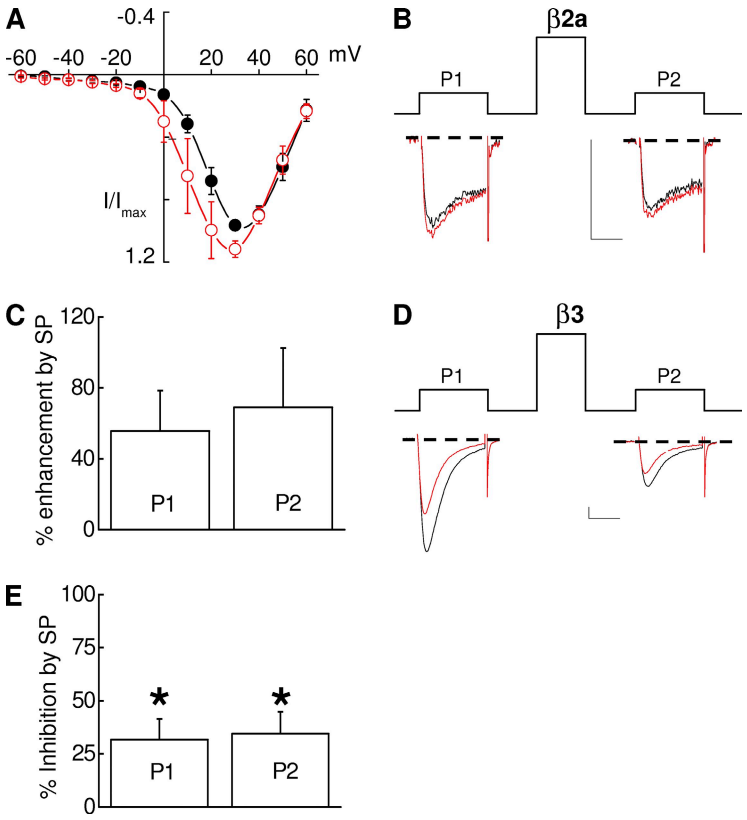


Figure 3. Modulation of Bdel1 current by SP is modestly disrupted. HEK-M1 cells were transiently transfected with NK-1R, Bdel1, $\alpha_2\delta$-1, β2a (A–C), or β3 (D and E). (A) Averaged current–voltage plots measured before and after application of SP (red). (B and C) Individual sweeps elicited at 20 mV (B) and summary of enhancement (C) taken before and 2 min after application of SP (red) before (P1) or after a prepulse (P2; $n = 7$). (D) Representative sweeps taken before and 2 min after application of SP. (E) Summary of the inhibition by SP at 20 mV caused by SP before (P1) and after a prepulse (P2; $n = 4$); *, $P < 0.05$ compared with control currents. Error bars represent SEM. Bars, 10 ms and 200 pA.

Indeed, SP inhibited currents of Bdel1/Ca_Vβ3 channels by 32 ± 10% ($P < 0.05$; Fig. 3, D and E). The magnitude of inhibition did not differ significantly from wt $Ca_V2.2$/β3 currents, indicating that the site of inhibition remained unaffected by the amino acid deletion in the IS6-AID segment. Moreover, no facilitation of modulated currents was observed with Bdel1 whether expressed with Ca_Vβ2a (Fig. 3, B and C) or Ca_Vβ3 (Fig. 3, D and E).

SP inhibits Bdel2 currents in the presence of palmitoylated β2a

To determine whether an additional amino acid deletion further alters N-current modulation, we tested the effects of SP on Bdel2 activity. We hypothesized that deletion of two amino acids (Fig. 1 D) might further displace Ca_Vβ2a from its normal position (Fig. 1 E), resulting in a more obvious disruption of N-current enhancement. After application of SP, robust inhibition of Bdel2 current was observed rather than enhancement (Fig. 4, A, B, and E). Inhibition was observed at all voltages (Fig. 4 A) and was not relieved by a prepulse (P1, 46 ± 7% vs. P2, 45 ± 8% at 10 mV). When inhibition of Bdel2/β2a currents was compared with inhibition of $Ca_V2.2$/β3 currents (Fig. 4, B and C), the magnitude of inhibition was similar and was not relieved by a prepulse (Fig. 4, D and E). Overall, current modulation by SP exhibited unique properties with each change in the orientation of Ca_Vβ2a: enhancement of N current, normally observed with $Ca_V2.2$/β2a channels, became more variable with Bdel1/β2a channels, whereas Bdel2/β2a currents exhibited robust inhibition similar to $Ca_V2.2$/β3 current modulation (Fig. 4 E).

It is unlikely that differences in modulation are caused by the loss of Ca_Vβ binding to Bdel1 because normally little to no current is observed when Ca_Vβ is left out of the transfection (Vitko et al., 2008). We also found that when Bdel2 was cotransfected with only $\alpha_2\delta$-1, mean current amplitude was −11 ± 7 pA ($n = 3$), indicating that to observe currents Ca_Vβ must be bound to channels. Additionally, to confirm that differences in modulation of Bdel mutants compared with wt $Ca_v2.2$ are not caused by the loss of Ca_Vβ expression, we performed BiFC analysis (Kerppola, 2006; Vitko et al., 2008) using Ca_Vβ2a coexpressed with $Ca_V2.2$, Bdel1, or Bdel2. This method utilizes CFP split into two nonfluorescent fragments: one fragment is fused to $Ca_V2.2$'s N terminus, and the other fragment is fused to Ca_Vβ2a's C terminus (Fig. S1 A). Fluorescence occurs when the two halves of CFP reside close enough to each other to bind, forming an intact fluorescing CFP. We found that each channel produced a fluorescent signal at the plasma membrane (Fig. S1 B), indicating that the differences in modulation were not caused by a loss of cell surface Ca_Vβ2a expression. These results differ from our previous study with β3 core (Vitko et al., 2008) because the CFP fragment was fused to a full-length β2a, which adds sufficient flexibility to allow BiFC regardless of orientation.

Downloaded from jgp.rupress.org on May 20, 2011

Published October 26, 2009

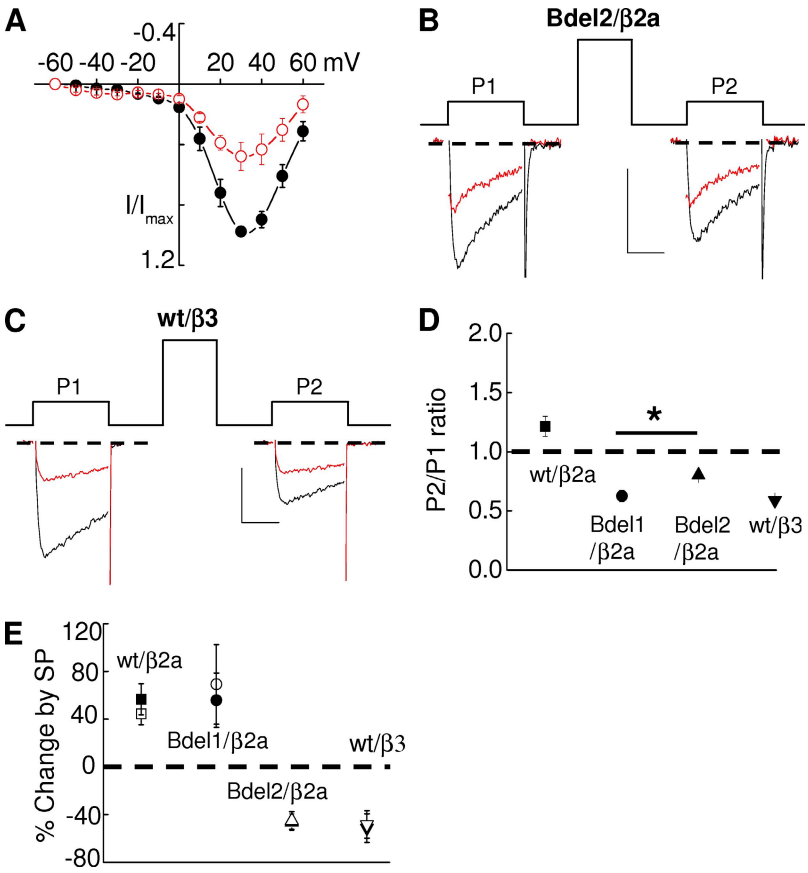


Figure 4. NK-1R activation inhibits Bdel2 currents. HEK-M1 cells were transiently transfected with Bdel2, $\alpha_2\delta$-1, $Ca_V\beta2a$, or $Ca_V\beta3$ and NK-1R. (A) Averaged current–voltage plot measured before and after application of SP. (B and C) Individual traces from $Ca_V\beta2a$-containing Bdel2 channels (B) or $Ca_V\beta3$-containing wt channels (C) taken before and 2 min after application of SP (red) before (P1) or after a prepulse (P2). (D) Prepulse facilitation (ratio of P2/P1) for wt $Ca_V2.2$ (■), Bdel1 (●), and Bdel2 with either $Ca_V\beta2a$ (▲) or $Ca_V\beta3$ (▼); *, $P < 0.05$ compared with Bdel1. (E) Summary of modulation of wt $Ca_V2.2$ (■), Bdel1 (●), and Bdel2 with either $Ca_V\beta2a$ (▲) or $Ca_V\beta3$ (▼) by SP before (closed) and after (open) a prepulse; *, $P < 0.05$ compared with control currents (n = 4–9). Error bars represent SEM. Bars, 10 ms and 200 pA.

To determine whether the amino acid deletions affect tonic facilitation of control currents, we measured the prepulse facilitation ratio, which is measured by the P2/P1 current amplitude ratio (Fig. 4, B–D). Although $Ca_V2.2$ currents showed small but significant prepulse facilitation (Fig. 4 D), both Bdel1 and Bdel2 currents decreased in amplitude after a prepulse. Interestingly, Bdel1 exhibited a significantly greater decrease in current amplitude after a prepulse than did Bdel2, resulting in a significantly ($P < 0.05$) lower P2/P1 current ratio for Bdel1 than Bdel2 (Fig. 4 D).

Inhibition of Bdel2/β2a currents by SP mimics inhibition of wt $Ca_v2.2/\beta3$ currents

By deleting two amino acids in the IS6-AID segment, N-current modulation changes from enhancement to robust inhibition. If the palmitoyl groups of $Ca_V\beta2a$ were critical for toggling modulation but are now displaced to reveal AA's inhibitory site on Bdel2, Bdel2/β2a inhibition should exhibit properties similar to Bdel2/β3 or $Ca_V2.2/\beta3$. Because Bdel2/β3 currents inactivate so rapidly, their peak current could not be compared with modulation of Bdel2/β2a currents (Vitko et al., 2008). Therefore, we took a pharmacological approach to determine whether the same slow pathway that inhibits $Ca_V2.2/\beta3$ currents confers Bdel2/β2a current inhibition. First, we tested whether inhibition of $Ca_V2.2/\beta3$ and Bdel2/β2a currents by SP occurs via a BAPTA-sensitive pathway (Beech et al., 1991; Bernheim et al., 1991; Mathie et al., 1992). When the normally low (0.1 mM) BAPTA concentration was raised to 20 mM BAPTA, N-current inhibition by SP was no longer significant for $Ca_V2.2/\beta3$ channels and was decreased with Bdel2/β2a channels (Fig. 5, compare A with B; and Fig. 5 E). Second, we tested whether BSA minimizes N-current inhibition by SP. Previously, we found that when BSA is included in the bath solution, inhibition of native and recombinant N current by M_1R stimulation is lost (Liu and Rittenhouse, 2003a; Liu et al., 2006; Heneghan et al., 2009). Because BSA sequesters free AA released from phospholipids (Fig. 5 C) after receptor activation (Liu et al., 2006), decreased N-current inhibition is attributed to decreased availability of free AA. When we tested both $Ca_V2.2/\beta3$ and Bdel2/β2a channels (Fig. 5, D and E) in the presence of BSA, N-current inhibition by SP was no longer observed.

Additionally, $Ca_V2.2/\beta3$ current inhibition by SP was not relieved by a prepulse (Fig. 4, D and E), consistent with inhibition occurring via a voltage-independent pathway (Kammermeier et al., 2000). Comparison of Bdel2/β2a and $Ca_V2.2/\beta3$ current inhibition (Fig. 4, B–E and Fig. 5 E) shows that for both currents, inhibition involves a voltage-independent, BAPTA-sensitive pathway that appears to use a free fatty acid, most likely AA, as a signaling

Downloaded from jgp.rupress.org on May 20, 2011

Published October 26, 2009

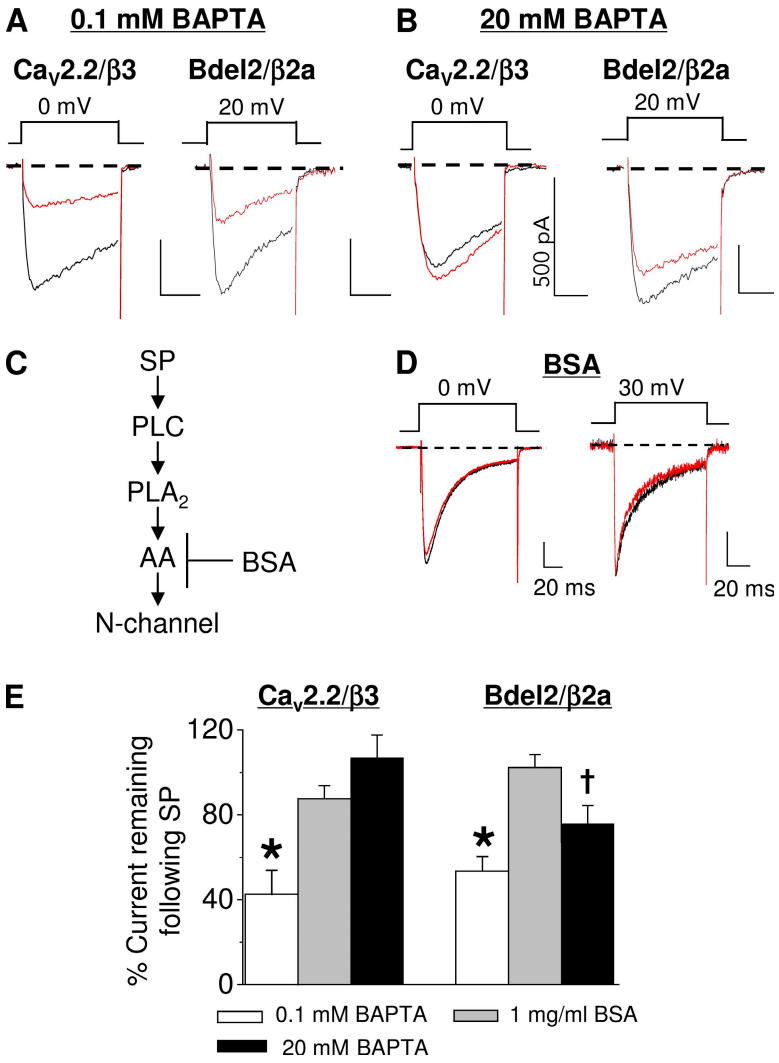


Figure 5. Bdel2 current inhibition by SP is voltage independent, BAPTA sensitive, and antagonized by BSA similar to slow pathway modulation of $Ca_V2.2$. HEK-M1 cells were transiently transfected with NK-1R, either Bdel2 or wt $Ca_V2.2$, $\alpha_2\delta$-1, and either $Ca_V\beta2a$ or $Ca_V\beta3$. (A and B) Individual traces from wt $Ca_V2.2/\beta3$ (left) and Bdel2/β2a currents (right) taken before and 90 s after application of SP with 0.1 mM BAPTA (A) or 20 mM BAPTA (B) in the pipette solution. (C) Schematic showing BSA's site of action. (D) 1 mg/ml BSA in the external bath medium. Left, wt $Ca_V2.2/\beta3$; right, Bdel2/β2a. (E) Summary of the percent current remaining after SP from $Ca_V2.2/\beta3$ and Bdel2/β2a channels; *, $P < 0.05$ compared with control currents ($n = 6$–9); †, $P < 0.05$ using a one-way paired t test compared with unstimulated current amplitudes. Error bars represent SEM. Bars, 10 ms and 200 pA.

molecule within the pathway. These findings are consistent with Bdel2/β2a current inhibition by SP occurring by a similar mechanism as $Ca_V2.2/\beta3$ current inhibition by the slow pathway (Fig. 1 A; Heneghan et al., 2009).

Free palmitic acid blocks inhibition of Bdel2 currents

In our companion study, exogenously applied palmitic acid blocked inhibition of $Ca_V2.2/\beta3$ currents by SP (Heneghan et al., 2009). If N-current inhibition of Bdel2/β2a and $Ca_V2.2/\beta3$ channels involves a similar pathway, exogenously applied palmitic acid also should minimize inhibition of Bdel2/β2a currents after SP application (Fig. 6 A). To test this hypothesis, cells expressing Bdel2 and $Ca_V\beta2a$ were preincubated with 10 µM palmitic acid for at least 8 min before application of SP. In the continued presence of palmitic acid, SP inhibited N current by 21 ± 4% (Fig. 6, C and D). This inhibition was significantly reduced ($P < 0.05$) by >50% compared with inhibition in the absence of palmitic acid (46 ± 7%; Fig. 6 D). These findings are consistent with a model in which the palmitoyl groups of $Ca_V\beta2a$ (Fig. 6 A) antagonize N-current inhibition by free AA that is released after SP application.

DISCUSSION

In our previous study, we found that coexpression of $Ca_V\beta2a$ with $Ca_V2.2$ and $\alpha_2\delta$-1 results in enhancement of recombinant N current by M_1R or NK-1R stimulation, whereas coexpression with $Ca_V\beta1b$, $Ca_V\beta3$, or $Ca_V\beta4$ results in inhibition (Heneghan et al., 2009). In the presence of $Ca_V\beta2a$, M_1R activation enhances native and recombinant N but not L current (Liu and Rittenhouse, 2003a; Liu et al., 2006; Heneghan et al., 2009; Roberts-Crowley and Rittenhouse, 2009). Additionally, enhancement of recombinant $Ca_V2.2$ and $Ca_V2.3$ currents by NK-1Rs has been described previously (Meza et al., 2007; Heneghan et al., 2009). Because these three channels show similar transmembrane organization (Catterall, 2000), the differences in modulation are unlikely to arise from nonspecific membrane effects that might alter gating. Additional studies using free palmitic acid, depalmitoylated $Ca_V\beta2a$, and chimeric $Ca_V\beta$s indicated that $Ca_V\beta2a$'s palmitoyl groups may confer the switch by blocking AA's inhibitory actions to reveal latent enhancement (Heneghan et al., 2009). In this study, we

Downloaded from jgp.rupress.org on May 20, 2011

Published October 26, 2009

manipulated the N-channel's pore-forming subunit $Ca_V2.2$ to alter $Ca_V\beta2a$'s orientation relative to $Ca_V2.2$. We hypothesized that one (Bdel1) or two (Bdel2) deletions in the rigid IS6-AID segment would displace $Ca_V\beta2a$ sufficiently from its normal orientation such that its palmitoyl groups no longer interact with the inhibitory site. Moreover, we predicted that with $Ca_V\beta2a$ reoriented, the N-current enhancement, normally observed after SP application, would be masked by rescued inhibition.

We found that deleting a single amino acid in the IS6-AID segment to form Bdel1 (Vitko et al., 2008) resulted in highly variable N-current enhancement of Bdel1/β2a channels (Fig. 3). Deleting two amino acids in the IS6-AID segment to form Bdel2 resulted in robust N-current inhibition replacing enhancement by SP (Fig. 4). In turn, preincubation with 10 µM palmitic acid minimized inhibition of Bdel2/β2a currents (Fig. 6), as was observed with wt $Ca_V2.2/\beta3$ currents (Heneghan et al., 2009), suggesting that the palmitoyl groups of $Ca_V\beta2a$ no longer reside in their wt position. Current inhibition of both $Ca_V2.2/\beta3$ and Bdel2/β2a channels (Figs. 4–5) exhibited similar properties to native N-current inhibition by the slow pathway in sympathetic neurons (Liu and Rittenhouse, 2003a), suggesting that displacement of $Ca_V\beta2a$ rescued inhibition mediated by phospholipid breakdown. These findings support a model in which $Ca_V\beta2a$'s palmitoyl groups may compete with and antagonize AA binding to a site on $Ca_V2.2$ that confers N-current inhibition by the slow pathway.

$Ca_V2.2/\beta2a$ current enhancement and Bdel2/β2a current inhibition both occur by a voltage-independent, BAPTA-sensitive pathway

Several of our findings advance the notion that the G_qPCRs NK-1R and M_1R use the same slow pathway to mediate both enhancement and inhibition (Fig. 1 A). First, both enhancement and inhibition of $Ca_V2.2$ currents by SP require low concentrations of BAPTA (0.1 mM) to observe modulation; the presence of 20 mM BAPTA in the pipette solution minimized modulation (Figs. 2 and 5). Native N-current inhibition by M_1Rs in SCG neurons (Beech et al., 1991; Bernheim et al., 1991; Mathie et al., 1992; Shapiro and Hille, 1993; Liu and Rittenhouse, 2003b) and hippocampal pyramidal neurons (Tai et al., 2006) and $Ca_V2.3$ current inhibition by NK-1Rs (Meza et al., 2007) are also BAPTA sensitive. Second, unlike membrane-delimited inhibition (De Waard et al., 2005), a prepulse preceding the test pulse has no effect on the magnitude of N-current enhancement (Fig. 2 B) or inhibition (Fig. 4 E) by SP. Both NK-1Rs and M_1Rs inhibit native N current via a voltage-independent pathway in SCG neurons (Beech et al., 1991; Mathie et al., 1992; Shapiro and Hille, 1993; Kammermeier et al., 2000; Liu and Rittenhouse, 2003b). Third, enhancement and inhibition exhibit similar pharmacological profiles. Preincubation of SCG neurons with the AA scavenger BSA or with the PLA_2 antagonist oleoyloxyethyl phosphorylcholine minimized enhancement and inhibition of native N current by M_1R agonists (Liu and Rittenhouse, 2003a). $Ca_V2.2$ current modulation by

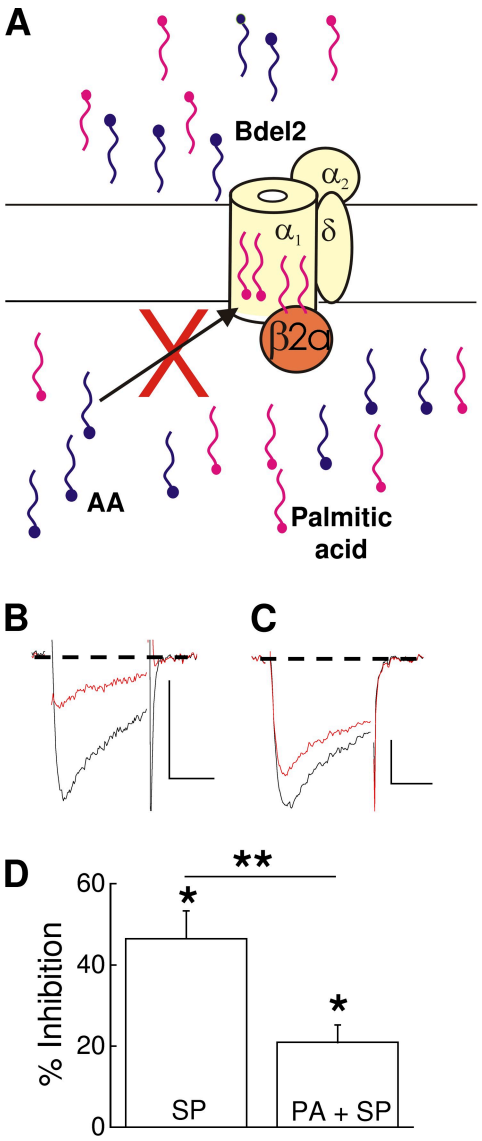


Figure 6. Exogenously applied palmitic acid blocks Bdel2 current inhibition by SP. HEK-M1 cells were transiently transfected with Bdel2, $\alpha_2\delta$-1, $Ca_V\beta2a$, and NK-1R. (A) Schematic representing preincubation of cells with 10 µM palmitic acid blocks free AA, released after stimulation of NK-1R, from occupying the inhibitory site. Enhancement site, not depicted. The two exogenous palmitic acids (magenta) are shown bound to the inner region of Bdel2, antagonizing AA from binding to the inhibitory sites. (B and C) Individual traces taken before and 2 min after application of 5 nM SP alone (B) or in the presence of 10 µM palmitic acid (C). (D) Summary of Bdel2 inhibition by SP in the presence of 10 µM palmitic acid (PA). *, $P < 0.05$ compared with current amplitude before SP ($n = 7$) or compared with the presence of palmitic acid alone ($n = 6$). **, $P < 0.05$; percent inhibition by SP compared with percent inhibition by palmitic acid + SP. Error bars represent SEM. Bars, 10 ms and 200 pA.

Downloaded from jgp.rupress.org on May 20, 2011

Published October 26, 2009

NK-1Rs exhibits these same two properties, whereas BSA (Fig. 5, D and E) and oleoyloxyethyl phosphorylcholine (not depicted) minimize both enhancement and inhibition. These findings suggest that although enhancement and inhibition may occur at distinct sites on N channels, they may be different manifestations of the same or overlapping signaling pathways. Thus, whether SP inhibits or enhances N current is determined by which $Ca_V\beta$ is coexpressed with $Ca_V2.2$ rather than from differences in signaling.

Further support for this idea comes from our finding that Bdel2/β2a channels exhibited N-current inhibition by SP similar to $Ca_V2.2/\beta3$ channels. Therefore, we attempted to determine whether this inhibition also was caused by the slow pathway. Coexpression of $Ca_V\beta2a$, compared with other $Ca_V\beta$s, results in increased prepulse-induced relief of tonic N-current inhibition and will undergo increased voltage-dependent, membrane-delimited inhibition by pertussis toxin–sensitive G proteins after stimulation of certain GPCRs (Cantí et al., 2000; Feng et al., 2001). Released $G\beta\gamma$ is thought to bind to the $Ca_V2.2$'s I–II linker, disrupting the association between the channel and $Ca_V\beta$ (Hümmer et al., 2003; De Waard et al., 2005). However, the inhibited Bdel2/β2a currents did not show voltage-dependent relief from inhibition after a prepulse in low BAPTA conditions (Fig. 4). Additionally, inhibition was decreased or lost when cells were either dialyzed with 20 mM BAPTA or when BSA was included in the bath solution, respectively. These characteristics of inhibition match slow pathway inhibition of N current observed in SCG neurons (Mathie et al., 1992; Shapiro and Hille, 1993; Liu and Rittenhouse, 2003a). The overlapping biophysical and pharmacological profile of modulation indicates that the same signaling pathway mediates N-current enhancement of $Ca_V2.2/\beta2a$ channels and inhibition of $Ca_V2.2/\beta3$ and Bdel2/β2a channels. Moreover, the observed enhancement of $Ca_V2.2/\beta2a$ versus inhibition of Bdel2/β2a channels suggests that changes in orientation of $Ca_V\beta2a$ underlie the switch in modulation. However, it was possible that $Ca_V\beta2a$ did not stay bound to Bdel2 and therefore was no longer present to block inhibition.

Bdel1 and Bdel2 alter $Ca_V\beta2a$'s position relative to the α1 subunit

Therefore, critical to understanding how the mutations in the IS6-AID segment disrupt enhancement was determining whether $Ca_V\beta2a$ remained associated with mutated N channels because β subunits appear able to dissociate from channels in the plasma membrane (Hidalgo et al., 2006; Hidalgo and Neely, 2007). Several pieces of data indicate that although Bdel1 and Bdel2 have a disrupted IS6-AID segment, $Ca_V\beta$ subunits continue to bind to $Ca_V2.2$. When β subunits are left out of the transfection protocol, <10% of the normal amount of current is detected with $Ca_V2.2$ (Cantí et al., 2001; Leroy et al., 2005), Bdel1 (Vitko et al., 2008), or Bdel2 (this study) even when T antigen is included. These observations, along with studies of other calcium channels (Singer et al., 1991; Wakamori et al., 1993), support the notion that to observe a robust current, a β subunit must be associated with the channel in mammalian cells. Our BiFC imaging data (Fig. S1) document that $Ca_V\beta2a$ binds to Bdel1 and Bdel2 at the plasma membrane. Because association of the two complementary parts of cerulean stabilizes the complex, the data cannot tell us whether $Ca_V\beta2a$ dissociates. However, in previous studies in which dissociation of β subunits was documented, reassociation was also detected (Hidalgo et al., 2006; Hidalgo and Neely, 2007), suggesting that if $Ca_V\beta2a$ can bind to $Ca_V2.2$, it will bind. Additional BiFC measurements of Bdel1 and Bdel2 coexpressed with a $Ca_V\beta$ core protein containing a truncated C terminus indicate that the β subunit is displaced relative to the pore in positions distinct from wt and from one another (Vitko et al., 2008).

Displacement of $Ca_V\beta2a$ from its normal orientation to $Ca_V2.2$ converts N-current enhancement to inhibition

The putative displacement of the palmitoyl groups may disrupt N-channel modulation by the slow pathway. With a single amino acid deletion in Bdel1, N current no longer exhibited significant enhancement by SP as a result of the increased variability of modulation. In contrast, when Bdel1 was coexpressed with $Ca_V\beta3$, SP significantly inhibited current, indicating that the inhibitory site on the α1 subunit remains functional. This latter finding rules out the possibility that disrupted gating underlies the increased variability in enhancement because Bdel1/$Ca_V\beta3$ channels also exhibit disrupted gating (Vitko et al., 2008) yet are inhibited by SP. Moreover, this finding indicates that the low-affinity interactions between $Ca_V\beta3$ and Bdel1 play at most a minor role in slow pathway inhibition of N current (He et al., 2007). Although the increased variability of Bdel1 current enhancement appears independent of altered protein–protein interactions, it is possible that the switch from current enhancement to inhibition for Bdel2 occurs as a result of changes in low-affinity interactions between $Ca_V\beta2a$ and Bdel2 arising from deletions in the I–II linker. However, we ruled out this possibility because exogenously applied palmitic acid significantly reduced current inhibition despite the novel orientation of $Ca_V\beta2a$ to Bdel2 (Fig. 6). Using a similar experimental design, we previously showed that exogenous application of palmitic acid blocked SP-mediated inhibition of $Ca_V2.2/\beta3$ currents (Heneghan et al., 2009). It is also unlikely that toggling from enhancement to inhibition occurs as a result of altered membrane curvature because the bulk concentration of phospholipids and fatty acids near the channel would not be expected to change despite the

Downloaded from jgp.rupress.org on May 20, 2011

Published October 26, 2009

reorientation of $Ca_V\beta2a$'s palmitoyl groups. Moreover, the BiFC images show that $Ca_V\beta2a$ is situated close to Bdel2 so that the endogenous palmitoyl groups should still reside extremely close to the channel. Thus, the switch from enhancement to inhibition after SP is most simply explained by a model in which the observed inhibition results from a loss of interaction by the displaced palmitoyl groups with the inhibitory site of Bdel2/$Ca_V\beta2a$ channels. The free palmitic acid then competes with endogenously released AA for the inhibitory site on the channel.

Although inhibition decreased with free palmitic acid, enhancement was not rescued. It is possible that the preincubation conditions were suboptimal for complete reversibility. However, palmitic acid will cross lipid bilayers within seconds with a permeability coefficient 400 times higher than that for water and diffusion rates 100 times faster than AA (Hamilton et al., 2002; Kamp and Hamilton, 2006). These biophysical properties of palmitic acid would suggest that its uptake into the membrane is not a limiting factor. Lastly, the choice of 10 µM palmitic acid seems appropriate because this concentration is within the measured physiological range (Vock et al., 2007). Notably, in pathophysiological conditions such as diabetic ketoacidosis, levels may rise up to 100 times this concentration (Smith et al., 1999). Thus, the lack of recovery of enhancement appears independent of the properties of exogenous free palmitic acid.

To minimize inhibition, we found that the $Ca_V\beta2a$ protein docks the palmitic acids while at the same time the palmitoyl groups hold the β subunit in a very specific orientation to $Ca_V2.2$. Our data would indicate that there is nothing casual about this interaction. Enhancement may also require specific protein–protein interactions because each $Ca_V\beta$ appears to establish a unique set of low-affinity interactions with $Ca_V2.2$ as well as bind to the AID (Qin et al., 1997; Walker and De Waard, 1998; Walker et al., 1998; Lao et al., 2008). Because all N channels appear capable of exhibiting enhancement, $Ca_V\beta$'s proper orientation to $Ca_V2.2$ through binding to the AID may somehow expose or stabilize the enhancement site. Because this orientation is disrupted with Bdel2, enhancement is also disrupted. Future studies with altered I–II linker sequence may resolve this question.

Physiological significance of N-channel regulation by palmitoylation

Mutations in the IS6-AID segment appear to disrupt critical protein–lipid interactions between the palmitoyl moieties of $Ca_V\beta2a$ and $Ca_V2.2$ that in turn uncouple the otherwise tight regulation of $Ca_V2.2$ by G_qPCRs. Entry of Ca^{2+} ions through N channels regulates the opening of small-conductance K^+_{Ca} channels during the posthyperpolarization (Stocker, 2004; Luther and Birren, 2006). N channels expressed postsynaptically on the dorsal horn affect neuronal excitability during and after transmission of nociceptive stimuli. Whether up- or down-regulation of the different Cavβs can occur in response to a nociceptive stimulus remains untested; however, both increases and decreases in Ca^{2+} currents have been observed in different neuronal subtypes after nerve injury (for review see McGivern and McDonough, 2004). Thus, any disruption in modulation of N current by SP (for example, during transmission of nociceptive stimulation) may alter the frequency of action potential firing in the spinal cord that conveys nociceptive information to the brain for further processing.

In summary, the data presented here, together with the findings of Heneghan et al. (2009), uncover a new function for protein palmitoylation. In addition to conferring unique gating properties, $Ca_V\beta2a$'s palmitoyl groups appear responsible for blocking inhibition to reveal enhancement by the slow pathway. In order for all of these processes to proceed normally, the palmitoylated $Ca_V\beta2a$ must be in a specific orientation. The precise docking of the palmitoyl groups allows $Ca_V\beta2a$ to effectively reach up into the membrane with its fatty acid "fingers" to alter $Ca_V2.2$'s gating properties and modulation. This new idea of a lipid modification of a cytosolic protein ($Ca_V\beta2a$) interacting with a transmembrane protein ($Ca_V2.2$) to change its regulation extends the role of palmitoylation beyond its known functions of targeting or tethering proteins to the membrane (Resh, 2006). Recently, Xue et al. (2004) made the novel observation that palmitoylation of a membrane-associated form of retinal epithelial protein 65 (RPE65) not only enhanced its targeting to membranes but most importantly enhanced its selectivity for binding to all-trans-retinyl-esters. However, these findings could be explained by a simple tethering mechanism for palmitoylation. Lastly, our findings predict that palmitoylation may confer to other cytoplasmic proteins the potential to interact with particular transmembrane proteins to alter their function.

We thank S. Ikeda, J. Jonassen, B. Kobertz, J. Lemos, and H.-S. Li for critically reading earlier versions of this manuscript. We thank D. Lipscombe for the $\alpha_1$2.2 cDNA. We also thank M.L. Roberts-Crowley, L. Liu, and A. Shchleglovitov for discussion and advice. T.-F. Chung (University of Massachusetts Medical School tissue culture facility) helped to maintain the HEK-M1 cell line.

This project was funded by the National Institutes of Health (grant NS34195 to A.R. Rittenhouse) and support from the University of Massachusetts Medical School and the University of Virginia Medical School.

Submitted: 20 January 2009
Accepted: 6 October 2009

REFERENCES

Barrett, C.F., L. Liu, and A.R. Rittenhouse. 2001. Arachidonic acid reversibly enhances N-type calcium current at an extracellular site. *Am. J. Physiol. Cell Physiol.* 280:C1306–C1318.

Beech, D.J., L. Bernheim, A. Mathie, and B. Hille. 1991. Intracellular Ca2+ buffers disrupt muscarinic suppression of Ca2+ current and

Downloaded from jgp.rupress.org on May 20, 2011

Published October 26, 2009

M current in rat sympathetic neurons. *Proc. Natl. Acad. Sci. USA.* 88:652–656. doi:10.1073/pnas.88.2.652

Bernheim, L., D.J. Beech, and B. Hille. 1991. A diffusible second messenger mediates one of the pathways coupling receptors to calcium channels in rat sympathetic neurons. *Neuron.* 6:859–867. doi:10.1016/0896-6273(91)90226-P

Cantí, C., Y. Bogdanov, and A.C. Dolphin. 2000. Interaction between G proteins and accessory subunits in the regulation of 1B calcium channels in *Xenopus* oocytes. *J. Physiol.* 527:419–432. doi:10.1111/j.1469-7793.2000.t01-1-00419.x

Cantí, C., A. Davies, N.S. Berrow, A.J. Butcher, K.M. Page, and A.C. Dolphin. 2001. Evidence for two concentration-dependent processes for beta-subunit effects on alpha1B calcium channels. *Biophys. J.* 81:1439–1451. doi:10.1016/S0006-3495(01)75799-2

Catterall, W.A. 2000. Structure and regulation of voltage-gated Ca2+ channels. *Annu. Rev. Cell Dev. Biol.* 16:521–555. doi:10.1146/annurev.cellbio.16.1.521

Chen, Y.H., M.H. Li, Y. Zhang, L.L. He, Y. Yamada, A. Fitzmaurice, Y. Shen, H. Zhang, L. Tong, and J. Yang. 2004. Structural basis of the alpha1-beta subunit interaction of voltage-gated Ca2+ channels. *Nature.* 429:675–680. doi:10.1038/nature02641

Chien, A.J., K.M. Carr, R.E. Shirokov, E. Rios, and M.M. Hosey. 1996. Identification of palmitoylation sites within the L-type calcium channel beta2a subunit and effects on channel function. *J. Biol. Chem.* 271:26465–26468. doi:10.1074/jbc.271.43.26465

Chien, A.J., T. Gao, E. Perez-Reyes, and M.M. Hosey. 1998. Membrane targeting of L-type calcium channels. Role of palmitoylation in the subcellular localization of the beta2a subunit. *J. Biol. Chem.* 273:23590–23597. doi:10.1074/jbc.273.36.23590

De Waard, M., J. Hering, N. Weiss, and A. Feltz. 2005. How do G proteins directly control neuronal Ca2+ channel function? *Trends Pharmacol. Sci.* 26:427–436. doi:10.1016/j.tips.2005.06.008

Feng, Z.P., M.I. Arnot, C.J. Doering, and G.W. Zamponi. 2001. Calcium channel beta subunits differentially regulate the inhibition of N-type channels by individual Gbeta isoforms. *J. Biol. Chem.* 276:45051–45058. doi:10.1074/jbc.M107784200

Gamper, N., V. Reznikov, Y. Yamada, J. Yang, and M.S. Shapiro. 2004. Phosphatidylinositol [correction] 4,5-bisphosphate signals underlie receptor-specific Gq/11-mediated modulation of N-type Ca2+ channels. *J. Neurosci.* 24:10980–10992. doi:10.1523/JNEUROSCI.3869-04.2004

Hamilton, J.A., W. Guo, and F. Kamp. 2002. Mechanism of cellular uptake of long-chain fatty acids: do we need cellular proteins? *Mol. Cell. Biochem.* 239:17–23. doi:10.1023/A:1020542220599

He, L.L., Y. Zhang, Y.H. Chen, Y. Yamada, and J. Yang. 2007. Functional modularity of the beta-subunit of voltage-gated Ca2+ channels. *Biophys. J.* 93:834–845. doi:10.1529/biophysj.106.101691

Heneghan, J.F., T. Mitra-Ganguli, L.F. Stanish, L. Liu, R. Zhao, and A.R. Rittenhouse. 2009. The Ca^{2+} channel β subunit determines whether stimulation of G_q-coupled receptors enhances or inhibits N current. *J. Gen. Physiol.* 134:369–384.

Hidalgo, P., and A. Neely. 2007. Multiplicity of protein interactions and functions of the voltage-gated calcium channel beta-subunit. *Cell Calcium.* 42:389–396. doi:10.1016/j.ceca.2007.05.009

Hidalgo, P., G. Gonzalez-Gutierrez, J. Garcia-Olivares, and A. Neely. 2006. The alpha1-beta-subunit interaction that modulates calcium channel activity is reversible and requires a competent alpha-interaction domain. *J. Biol. Chem.* 281:24104–24110. doi:10.1074/jbc.M605930200

Hümmer, A., O. Delzeith, S.R. Gomez, R.L. Moreno, M.D. Mark, and S. Herlitze. 2003. Competitive and synergistic interactions of G protein beta(2) and Ca(2+) channel beta(1b) subunits with Ca(v)2.1 channels, revealed by mammalian two-hybrid and fluorescence resonance energy transfer measurements. *J. Biol. Chem.* 278:49386–49400. doi:10.1074/jbc.M306645200

Kammermeier, P.J., V. Ruiz-Velasco, and S.R. Ikeda. 2000. A voltage-independent calcium current inhibitory pathway activated by muscarinic agonists in rat sympathetic neurons requires both Galpha q/11 and Gbeta gamma. *J. Neurosci.* 20:5623–5629.

Kamp, F., and J.A. Hamilton. 2006. How fatty acids of different chain length enter and leave cells by free diffusion. *Prostaglandins Leukot. Essent. Fatty Acids.* 75:149–159. doi:10.1016/j.plefa.2006.05.003

Kerppola, T.K. 2006. Design and implementation of bimolecular fluorescence complementation (BiFC) assays for the visualization of protein interactions in living cells. *Nat. Protoc.* 1:1278–1286. doi:10.1038/nprot.2006.201

Lao, Q.Z., E. Kobrinsky, J.B. Harry, A. Ravindran, and N.M. Soldatov. 2008. New determinant for the CaVbeta2 subunit modulation of the CaV1.2 calcium channel. *J. Biol. Chem.* 283:15577–15588. doi:10.1074/jbc.M802035200

Leroy, J., M.S. Richards, A.J. Butcher, M. Nieto-Rostro, W.S. Pratt, A. Davies, and A.C. Dolphin. 2005. Interaction via a key tryptophan in the I-II linker of N-type calcium channels is required for beta1 but not for palmitoylated beta2, implicating an additional binding site in the regulation of channel voltage-dependent properties. *J. Neurosci.* 25:6984–6996. doi:10.1523/JNEUROSCI.1137-05.2005

Lin, Z., S. Haus, J. Edgerton, and D. Lipscombe. 1997. Identification of functionally distinct isoforms of the N-type Ca2+ channel in rat sympathetic ganglia and brain. *Neuron.* 18:153–166. doi:10.1016/S0896-6273(01)80054-4

Liu, L., and A.R. Rittenhouse. 2003a. Arachidonic acid mediates muscarinic inhibition and enhancement of N-type Ca2+ current in sympathetic neurons. *Proc. Natl. Acad. Sci. USA.* 100:295–300. doi:10.1073/pnas.0136826100

Liu, L., and A.R. Rittenhouse. 2003b. Pharmacological discrimination between muscarinic receptor signal transduction cascades with bethanechol chloride. *Br. J. Pharmacol.* 138:1259–1270. doi:10.1038/sj.bjp.0705157

Liu, L., C.F. Barrett, and A.R. Rittenhouse. 2001. Arachidonic acid both inhibits and enhances whole cell calcium currents in rat sympathetic neurons. *Am. J. Physiol. Cell Physiol.* 280:C1293–C1305.

Liu, L., R. Zhao, Y. Bai, L.F. Stanish, J.E. Evans, M.J. Sanderson, J.V. Bonventre, and A.R. Rittenhouse. 2006. M1 muscarinic receptors inhibit L-type Ca2+ current and M-current by divergent signal transduction cascades. *J. Neurosci.* 26:11588–11598. doi:10.1523/JNEUROSCI.2102-06.2006

Luther, J.A., and S.J. Birren. 2006. Nerve growth factor decreases potassium currents and alters repetitive firing in rat sympathetic neurons. *J. Neurophysiol.* 96:946–958. doi:10.1152/jn.01078.2005

Mathie, A., L. Bernheim, and B. Hille. 1992. Inhibition of N- and L-type calcium channels by muscarinic receptor activation in rat sympathetic neurons. *Neuron.* 8:907–914. doi:10.1016/0896-6273(92)90205-R

McGivern, J.G., and S.I. McDonough. 2004. Voltage-gated calcium channels as targets for the treatment of chronic pain. *Curr. Drug Target. CNS Neurol. Disord.* 3:457–478.

Meza, U., A. Thapliyal, R.A. Bannister, and B.A. Adams. 2007. Neurokinin 1 receptors trigger overlapping stimulation and inhibition of CaV2.3 (R-type) calcium channels. *Mol. Pharmacol.* 71:284–293. doi:10.1124/mol.106.028530

Opatowsky, Y., O. Chomsky-Hecht, and J.A. Hirsch. 2004. Expression, purification and crystallization of a functional core of the voltage-dependent calcium channel beta subunit. *Acta Crystallogr. D Biol. Crystallogr.* 60:1301–1303. doi:10.1107/S0907444904010686

Pragnell, M., M. De Waard, Y. Mori, T. Tanabe, T.P. Snutch, and K.P. Campbell. 1994. Calcium channel beta-subunit binds to a conserved motif in the I-II cytoplasmic linker of the alpha 1-subunit. *Nature.* 368:67–70. doi:10.1038/368067a0

Qin, N., D. Platano, R. Olcese, E. Stefani, and L. Birnbaumer. 1997. Direct interaction of gbetagamma with a C-terminal

Downloaded from jgp.rupress.org on May 20, 2011

Published October 26, 2009

gbetagamma-binding domain of the Ca2+ channel alpha1 subunit is responsible for channel inhibition by G protein-coupled receptors. *Proc. Natl. Acad. Sci. USA.* 94:8866–8871. doi:10.1073/pnas.94.16.8866

Resh, M.D. 2006. Palmitoylation of ligands, receptors, and intracellular signaling molecules. *Sci. STKE.* doi:10.1126/stke.3592006re14

Roberts-Crowley, M.L., and A.R. Rittenhouse. 2009. Arachidonic acid inhibition of L-type calcium (CaV1.3b) channels varies with accessory CaVβ subunits. *J. Gen. Physiol.* 133:387–403. doi:10.1085/jgp.200810047

Shapiro, M.S., and B. Hille. 1993. Substance P and somatostatin inhibit calcium channels in rat sympathetic neurons via different G protein pathways. *Neuron.* 10:11–20. doi:10.1016/0896-6273(93)90237-L

Singer, D., M. Biel, I. Lotan, V. Flockerzi, F. Hofmann, and N. Dascal. 1991. The roles of the subunits in the function of the calcium channel. *Science.* 253:1553–1557. doi:10.1126/science.1716787

Smith, J.M., S.M. Solar, D.J. Paulson, N.M. Hill, and T.L. Broderick. 1999. Effect of palmitate on carbohydrate utilization and Na/K-ATPase activity in aortic vascular smooth muscle from diabetic rats. *Mol. Cell. Biochem.* 194:125–132. doi:10.1023/A:1006961005422

Stocker, M. 2004. Ca(2+)-activated K+ channels: molecular determinants and function of the SK family. *Nat. Rev. Neurosci.* 5:758–770. doi:10.1038/nrn1516

Tai, C., J.B. Kuzmiski, and B.A. MacVicar. 2006. Muscarinic enhancement of R-type calcium currents in hippocampal CA1 pyramidal neurons. *J. Neurosci.* 26:6249–6258. doi:10.1523/JNEUROSCI.1009-06.2006

Takahashi, S.X., S. Mittman, and H.M. Colecraft. 2003. Distinctive modulatory effects of five human auxiliary beta2 subunit splice variants on L-type calcium channel gating. *Biophys. J.* 84:3007–3021. doi:10.1016/S0006-3495(03)70027-7

Van Petegem, F.K., K.A. Clark, F.C. Chatelain, and D.L. Minor Jr. 2004. Structure of a complex between a voltage-gated calcium channel beta-subunit and an alpha-subunit domain. *Nature.* 429:671–675. doi:10.1038/nature02588

Vitko, I., I. Bidaud, J.M. Arias, A. Mezghrani, P. Lory, and E. Perez-Reyes. 2007. The I-II loop controls plasma membrane expression and gating of Ca(v)3.2 T-type Ca2+ channels: a paradigm for childhood absence epilepsy mutations. *J. Neurosci.* 27:322–330. doi:10.1523/JNEUROSCI.1817-06.2007

Vitko, I., A. Shcheglovitov, J.P. Baumgart, I.I. Arias-Olguín, J. Murbartián, J.M. Arias, and E. Perez-Reyes. 2008. Orientation of the calcium channel beta relative to the alpha(1)2.2 subunit is critical for its regulation of channel activity. *PLoS One.* 3:e3560. doi:10.1371/journal.pone.0003560

Vock, C., M. Gleissner, F. Klapper, and F. Doring. 2007. Identification of palmitate-regulated genes in HepG2 cells by applying microarray analysis. *Biochim. Biophys. Acta.* 1770:1283–1288.

Wakamori, M., G. Mikala, A. Schwartz, and A. Yatani. 1993. Single-channel analysis of a cloned human heart L-type Ca2+ channel alpha 1 subunit and the effects of a cardiac beta subunit. *Biochem. Biophys. Res. Commun.* 196:1170–1176. doi:10.1006/bbrc.1993.2374

Walker, D., and M. De Waard. 1998. Subunit interaction sites in voltage-dependent Ca2+ channels: role in channel function. *Trends Neurosci.* 21:148–154. doi:10.1016/S0166-2236(97)01200-9

Walker, D., D. Bichet, K.P. Campbell, and M. De Waard. 1998. A beta 4 isoform-specific interaction site in the carboxyl-terminal region of the voltage-dependent Ca2+ channel alpha 1A subunit. *J. Biol. Chem.* 273:2361–2367. doi:10.1074/jbc.273.4.2361

Wu, L., C.S. Bauer, X.G. Zhen, C. Xie, and J. Yang. 2002. Dual regulation of voltage-gated calcium channels by PtdIns(4,5)P2. *Nature.* 419:947–952. doi:10.1038/nature01118

Xue, L., D.R. Gollapalli, P. Maiti, W.J. Jahng, and R.R. Rando. 2004. A palmitoylation switch mechanism in the regulation of the visual cycle. *Cell.* 117:761–771. doi:10.1016/j.cell.2004.05.016

Zhang, Y., Y.H. Chen, S.D. Bangaru, L. He, K. Abele, S. Tanabe, T. Kozasa, and J. Yang. 2008. Origin of the voltage dependence of G-protein regulation of P/Q-type Ca2+ channels. *J. Neurosci.* 28:14176–14188. doi:10.1523/JNEUROSCI.1350-08.2008

Downloaded from jgp.rupress.org on May 20, 2011